Romanian Reports in Physics, Vol. 59, No. 2, P. 419–431, 2007

Dedicated to Prof. Dorin N. Poenaru's 70th Anniversary

MEDIUM DEPENDENCE OF VECTOR MESON PROPERTIES IN HEAVY ION COLLISIONS

AMAND FAESSLER, CHRISTIAN FUCHS

Institute for Theoretical Physics, University of Tuebingen, 72076 Tuebingen, Germany

(Received December 24, 2006)

Abstract. Heavy ion collisions produce dense and hot nuclear matter. Dileptons give information about this hot and dense phase. The dileptons are produced by vector mesons. Theoretical calculation of dilepton production in the DLS (Berkeley), the HADES (GSI) experiments and the CERES, HELIOS and NA60 data from CERN give information about possible modifications of the vector meson properties in hot and dense nuclear matter. Here the description in relativistic quantum molecular dynamics of heavy ion collisions and dilepton production are presented and compared with data.

Key words: heavy ion collisions; dense and hot nuclear matter; dileptons; medium dependence.

1. INTRODUCTION

For the study of nuclear matter under extreme conditions, heavy ion reactions present a unique opportunity allowing a comprehensive analysis of the phase structure of the underlying theory of strong interactions. In this process electromagnetic probes such as dileptons have been proven to be most effective since they leave the reaction zone essentially undistorted by final state interactions. They provide thus a clear view on effective degrees of freedom at high baryon density and temperature. It has been argued that their differential spectra could reveal information about chiral restoration and in-medium properties of hadrons [1, 2, 3]. Theoretically, there exists an abundance of models that predict a change of vector meson masses and widths in high density/temperature nuclear matter: Brown-Rho scaling [1] is equivalent with a decrease of vector meson masses in nuclear medium; models based on QCD sum rules [2] and effective hadronis models [4, 5] reach similar conclusions.

Experimentally, dilepton spectra have been measured at two different energy regimes: the CERES [6, 7], HELIOS [8] and recently NA60 [9] at CERN have measured dielectrons and dimuons, respectively, in heavy ion reactions at 158 GeV/nucleon. In proton-nucleus reactions as well as in heavy ion reactions of light systems (S+W) the sum over all measured hadronic sources, i.e. the so-called hadronic cocktail, describes the corresponding dilepton spectra perfectly well. However, in heavy systems (Pb+Au) a significant enhancement of the dilepton spectra below the ρ and ω peaks has been observed relative to the corresponding hadronic cocktail. Such a behavior could be explained theoretically, within a scenario of a dropping ρ vector meson mass [10] or by the inclusion of in-medium spectral functions for the vector mesons [11, 12]. The recent NA60 dimuon spectra with high resolution in the vicinity around the $\rho - \omega$ peak seem to rule out a naive dropping mass scenario but support the picture of modified $\rho - \omega$ spectral functions. An enhanced strength below the ω peak has also been observed in γ-nucleus reactions [13]. A second set of heavy ion experiments have been performed at laboratory energies of 1.0 AGeV (Ca+Ca and C+C) by the DLS Collaboration at BEVALAC [14, 15]. Also in this case, the low mass region of the dilepton spectra is underestimated by present transport calculations, in contrast with similar measurements (1.04 - 4.88 GeV/nucleon) for the p+p and p+d systems. As opposed to the ultra-relativistic case, the situation does not improve when the in-medium spectral functions or the dropping mass scenarios are taken into account [12, 16] (the DSL puzzle). Other scenarios like possible contributions from the quark-gluon plasma or in-medium modifications of the η mass have been excluded as a possible resolution of this puzzle. Decoherence effects [17] have been proven to be partially successful in explaining the difference between the DLS data and the theoretical predictions.

Recently, a new measurement by the HADES Collaboration at GSI has been completed and the results will be published in the near future [18]. The aim of this second generation experiment is to measure dilepton spectra in A+A, p+A and π+A reactions with an unprecedented mass resolution ($\Delta M/M \simeq 1\%(\sigma)$) over the entire spectrum [19]. Such a resolution allows to measure the in-medium properties (mass and width) of ρ and ω mesons through their decays into dielectron pairs in nuclear matter with high precision and will put strong constraints on theoretical models. This letter prevents predictions of the dilepton production in C+C reactions at 1.0 and 2.0 AGeV which are those reactions where first data from HADES will be available in the near future. The vector meson and dilepton production is described within the framework of the resonance model developed in [20, 21, 22] in combination with the relativistic quantum molecular dynamics (RQMD) transport model for heavy ion collisions [17]. The influence of medium effects such as quantum

decoherence, collisional broadening and a dropping vector meson mass are investigated. The paper is organized as follows: in Section 2 we give a brief description of the elementary reactions which contribute to dilepton emission in heavy ion collisions, together with an outline of the RQMD model. Section 3 is devoted to the presentation of our prediction for the differential mass spectrum of dilepton production in 1.0 and 2.0 AGeV C+C collisions.

2. ELEMENTARY DILEPTON SOURCES

The elementary sources of dilepton production in heavy ion reaction in the energy range of a few GeV/nucleon are numerous. One can identify three main classes of processes that lead to dilepton emission: nucleon-nucleon bremsstrahlung, decays of light unflavored mesons and decays of nucleon and Δ resonances. For the energy range of interest in this paper dilepton generation through nucleon-nucleon bremsstrahlung is unimportant. Feynman diagrams of processes belonging to the last two classes are depicted in 1.

At incident energies of 1 AGeV the cross-sections for meson production $\mathcal{M} = \eta, \eta', \rho, \omega, \phi$ are small and these mesons do not play an important role in the dynamics of heavy-ion collisions. Their production can thus be treated perturbatively, in contrast to the case of the pion. The decay to a dilepton pair takes place through the emission of a virtual photon. The differential branching ratios for the decay of a meson to a final state Xe^+e^- can be written

$$dB(\mu, M)^{\mathcal{M},\pi\to e^+e^-X} = \frac{d\Gamma(\mu, M)^{\mathcal{M},\pi\to e^+e^-X}}{\Gamma_{tot}^{\mathcal{M},\pi}(\mu)}, \tag{1}$$

with μ the meson mass and M the dilepton mass. Three types of such decays have been considered: direct decays $\mathcal{M} \to e^+e^-$ (Fig. 1a), Dalitz decays $\mathcal{M} \to \gamma e^+e^-$, $\mathcal{M} \to \pi(\eta)e^+e^-$ (Fig. 1b) and four-body decays $\mathcal{M} \to \pi\pi e^+e^-$ (Fig. 1c). A comprehensive study of the decay of light mesons to a dilepton pair has been performed in [20], the decay channels there are most important quantitatively for heavy-ion collisions at 1 and 2 GeV/nucleon being $\pi^0 \to \gamma e^+e^-$ and $\eta \to \gamma e^+e^-$.

The third source for dilepton emission we have mentioned was the decay of baryonic resonances (Fig. 1d). For the description of this process an extension of the vector meson dominance (VMD) model has been employed [20, 21]. The original VMD model assumes that decays of baryon resonances run through an intermediate virtual meson (ρ or ω) required for the description of the form-factors entering in the calculation of the radiative ($R \to N\gamma$) and mesonic ($R \to NV$) decays. Such a model does not allow the simultaneous description of both radiative and mesonic decays [5, 22, 23]. Furthermore the quark counting rules require a stronger suppression of the

transition form-factor than the $1/t$ behavior predicted by the naive VMD. Similarly the $\omega\pi\gamma$ transition form-factor shows an asymptotic $1/t^2$ behavior [24]. An extension of the VMD to allow contributions from radially excited vector mesons ($\rho(1250)$, $\rho(1450)$, ... in Ref. [21]) that interfere destructively with the ground state vector mesons (ρ in this example) allow for a resolution of the mentioned problems of the original VMD and describe the radiative and mesonic decays in a unitary way.

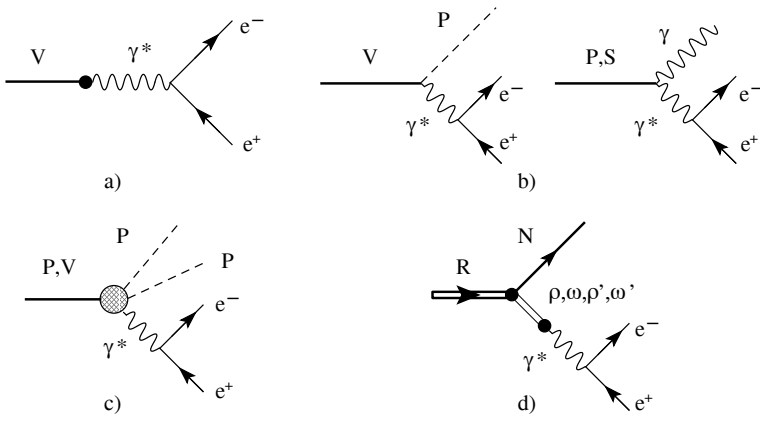

Fig. 1 – Feynman diagrams of the elementary processes contributing emission: a) direct decay of a vector meson (ρ, ω, ϕ) to a dilepton pair going through an intermediate photon (VMD model); b) Dalitz decays of a vector (V), pseudo-scalar (P) or scalar meson (S) into a dilepton pair and a photon or a pseudo-scalar meson (η or π); c) four-body decay into a dilepton pair plus two pseudo-scalar mesons (the hashed vertex represents an intermediate state containing a vector meson and/or virtual photon = see Ref. [20]); d) the decay of a nucleon or Δ resonance into a nucleon plus a virtual vector meson (extended VMD) which then decays into two dileptons.

In terms of the branching ratios for the Dalitz decays of the baryon resonances, the cross section for e^+e^- production from the initial state X' together with the final state NX can be written

$$\frac{d\sigma(s,M)^{X'\to NXe^+e^-}}{dM^2} = \sum_R \int_{(m_N+M)^2}^{\sqrt{s}-m_X)^2} d\mu^2 \times \frac{d\sigma(s,\mu)^{X'\to RX}}{d\mu^2} \sum_V \frac{dB(\mu,M)^{R\to VN\to Ne^+e^-}}{dM^2}\,, \tag{2}$$

where μ is the mass of the baryon resonance R which has the production cross-section $d\sigma(s,\mu)^{X'\to XR}$ and $dB(\mu,M)^{R\to VN\to e^+e^-}$ being the differential branching ratio for the decay of the resonance $R \to Ne^+e^-$ through the

vector meson V. The initial state X' could consist of two baryons ($X' = NN, NR, RR'$) or of one nucleon and a pion ($X = \pi N$). The dilepton decay rate can be found, once the width $\Gamma(R \to N\gamma^*)$ is known by using the factorisation prescription

$$d\Gamma(R \to Ne^+e^-) = \Gamma(R \to N\gamma^*)\, M\, \Gamma(\gamma^* \to e^+e^-)\, \frac{dM^2}{\pi M^4}\,, \tag{3}$$

with

$$M\Gamma(\gamma^* \to e^+e^-) = \frac{\alpha}{3}\,(M^2 + 2m_e^2)\,\sqrt{1 - \frac{4m_e^2}{M^2}}\,. \tag{4}$$

The decay width $\Gamma(R \to N\gamma^*)$ is described within the extended VMD model [21] in terms of three transition form-factors (magnetic, electric and Coulomb) in case of a resonance with spin $J > 1/2$ and two for $J = 1/2$, which is just the number of independent helicity amplitudes for the respective spin value. The free parameters of the model are fixed by constraining the asymptotic form of the form-factors by quark counting rules [25] and fitting to the experimental data for photo-production and electro-production amplitudes and partial-wave analysis for multichannel πN scattering. The number of intermediate ρ or ω states required to describe the transition form-factors depends on the spin J of the resonance in question: namely $J - 1/2 + 3$. For the case that $J_{max} = 7/2$ one needs 6 intermediate mesons, with the masses chosen as follows: 0.769, 1.250, 1.450, 1.720, 2.150 and 2.350 (in GeV). Within this model a consistent description of radiative and mesonic decays could be achieved. Further details about the extended VDM can be found in [21]. Figure 2 shows the ω production in elmentary NN reactions. The different cross sections are shown as functions of the excess energy ϵ. As discussed in [26], the resonance model (with a large $N^*(1535)N\omega$ coupling) leads to very accurate description of the measured on-shell cross section. It has, however, a very strong off-shell component which fully contributes to the dilepton production. The weak coupling scenario, on the other side, has only small off-shell component but the reproduction of the data is relatively poor in the low energy regime. In [28] it has finally been demonstrated that the resonance model is able to describe the measured ω- and ϕ-meson angular distributions in proton-proton reactions.

Before turning to heavy ion collisions we will consider the dilepton production in elementary reactions. Dilepton spectra in proton-proton and proton deuteron reactions have been measured by the DLS Collaboration in the energy range from $T = 1 \div 5$ GeV [15]. The application of the present model to the dilepton production in *pp* reactions has in detail been discussed in [22]. For completeness we show the corresponding results and the comparison to the DLS data [15] in Fig. 3. The agreement with the available data is generally reasonable, i.e. of similar quality as obtained in previous calculations by

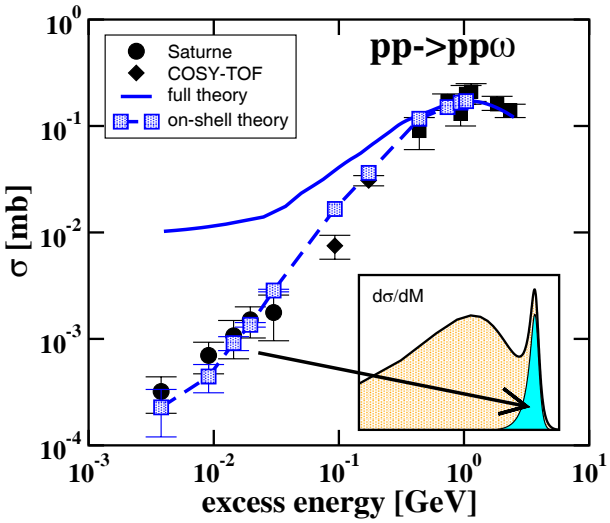

Fig. 2 – Exclusive $pp \to pp\omega$ cross section obtained in the resonance model as a function of the excess energy ϵ. The solid curve shows the full cross section including off-shell contributions while the squares show the experimentally detectable on-shell part of the cross section. Data are taken from [27].

Ernst et al. [29] and Bratkovskaja et al. [30]. As in [29] we observe a slight underestimation of the experimental dilepton yield at the two highest energies $T = 2.09$ and 4.88 GeV in the mass region below the $\rho - \omega$ peak. Here the knowledge of the inclusive cross section with multi-pion final channels starts to play an important role. In [22] the multi-pion production was estimated within a semi-empirical model which is slightly modified in the present case. However, results are very similar to our previous calculations [22].

It should be noted that the dilepton yields in pp reactions were obtained with the strong $N^*(1535) - N\omega$ decay mode. As in detail discussed in [26] the strong coupling mode is the result of the eVMD fit to the available photo- and meson-production data [21]. It leads to sizeable contributions from off-shell ω production around threshold energies which are, however, experimentally not accessible in $pp \to pp\omega$ measurements. On the other side, these off-shell ω's fully contribute to the dilepton yield. The off-shell contributions lead generally to an enhancement of the dilepton yield in the mass region below the ω peak, in particular at incident energies where the ω is dominantly produced subthreshold. In contrast to [29, 30] where the ω is treated as an elementary particle (with fixed mass $m_\omega = 782$ MeV) in our approach the off-shell ω production starts at the three-pion threshold. Thus subthreshold ω production appears already in elementary reactions. As can be seen from Fig. 3 the scenario of large off-shell ω contributions which are the consequence of

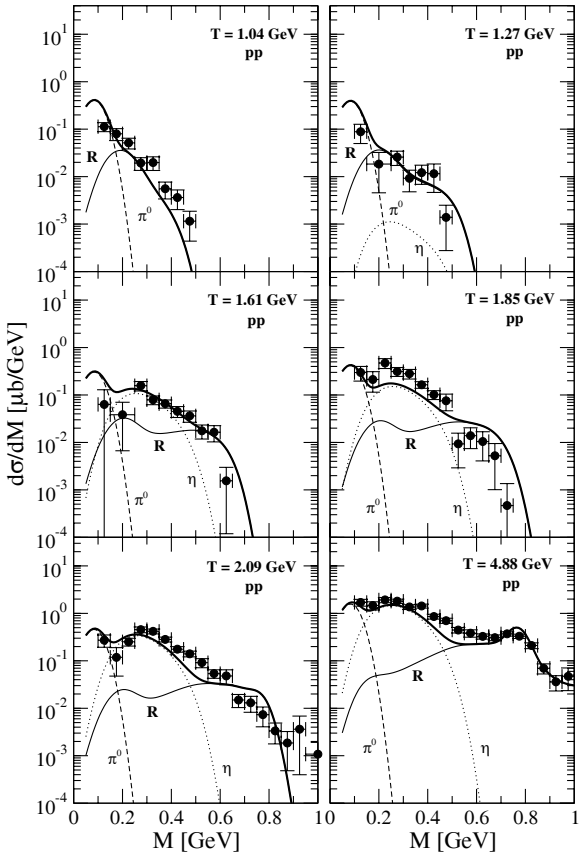

Fig. 3 – The differential $pp \to e^+e^-X$ cross sections at various proton kinetic energies are compared to the DLS data [15].

the strong $N^*(1535) - N\omega$ coupling are consistent with the experimental pp dilepton yields in the energy range of $T = 1.04 \div 1.61$ GeV. At higher energies this off-shell production becomes negligible [26].

3. HEAVY ION REACTIONS

As already mentioned the decay widths $\Gamma(R \to N\gamma^*)$ are expressed in terms of the magnetic, electric and Coulomb form-factors, more precisely they depend on the modulus squared of these form-factors. In the extended VMD each of these form-factors is in turn expressed as a linear superposition of the contributions from the intermediate vector mesons (ρ or ω):

$$G_T^{(\pm)}(M^2) = \sum_k \mathcal{M}_{Tk}^{(\pm)}, \tag{5}$$

with T standing for each of possible form-factors, $(\pm)$ denotes states of normal and abnormal parity respectively and the sum is over the intermediate mesons. The amplitude

$$\mathcal{M}_{Tk}^{(\pm)} = h_{Tk}^{(\pm)} \frac{m_k^2}{m_k^2 - i m_k \Gamma_k - M^2} \tag{6}$$

represents the contribution of the k^{th} vector meson to the amplitude of type T. The residues $h_{Tk}^{(\pm)}$ are fixed by the requirement that the asymptotic expression of the form-factors is consistent with the quark counting rules [25]. This leads to a destructive interference between the intermediate vector mesons, since quark counting rules predict a behavior steeper for the form-factors than the $1/M^2$ contribution of a single meson. In the medium it is expected that the coherence between the contributions of individual mesons is at least partially lost. In the extreme case of total decoherence, this would lead to the following replacement in the expression for the decay width,

$$\Big| \sum_k \mathcal{M}_{Tk}^{(\pm)} \Big|^2 \longrightarrow \sum_k \left| \mathcal{M}_{Tk}^{(\pm)} \right|^2 , \tag{7}$$

which will result in an enhancement of the resonance contributions. In reality both, the density and wavelength of the meson are finite. Introducing the decay length L_D of a resonance and its collision length L_C one can determine the probability of coherent decay (i.e. the meson decay takes place before the first collision) as $w = \frac{L_C}{L_C + L_C}$. In order to account for the decoherence effect, one can introduce an enhancement factor $E_T(M^2, \vec{Q}^2)$,

$$\left| G_T^{(\pm)}(M^2) \right|^2 \longrightarrow E_T^{(\pm)}(M^2, \vec{Q}^2) \left| G_T^{(\pm)}(M^2) \right|^2 . \tag{8}$$

The dependence on the space-like part $\vec{Q}$ of the vector meson momentum originates from the definition of the collision length L_C. Further details can be found in Ref. [17].

Although the present model is able to reproduce the vector meson and the dilepton production in elementary reactions with high precision the situation in unsatisfactory when turning to heavy ion collisions. Heavy ion collisions are described within the QMD transport model [17]. Without additional in-medium effect we observe in two distinct kinematical regions significant deviations from the dilepton yields measured by the DLS Collaboration in C+C and Ca+Ca reactions at 1 AGeV. As can be seen from Fig. 4 at small invariant masses the experimental data are strongly underestimated which confirms the observations made by other groups [29, 31]. Although accounting for the experimental resolution we observe further a clear structure of the ρ/ω peak which is not present in the data.The collisional broadening of the vector mesons suppresses the ρ/ω peak in the dilepton spectra. This allows

to extract empirical values for the in-medium widths of the vector mesons. From the reproduction of the DLS data the following estimates for the collision widths $\Gamma_\rho^{\rm coll} = 150$ MeV and $\Gamma_\omega^{\rm coll} = 100 - 300$ MeV can be made. The in-medium values correspond to an average nuclear density of about 1.5 ρ_0 and have been used in the calculation shown in Fig. 3.

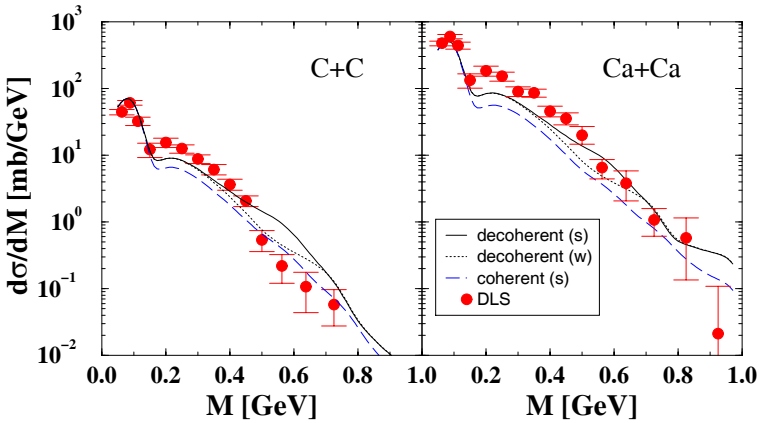

Fig. 4 – Influence of the microscopically determined decoherent dilepton emission in C+C and Ca+Ca reactions. A strong (s), respectively, weak (w) $N^*(1535) - N\omega$ coupling is used. For comparison also the coherent case (s) is shown. Data are from the DLS Collaboration [15].

The second medium effect discussed in [17] concerns the problem of quantum interference. Semi-classical transport models like QMD do generally not account for interference effects, i.e. they propagate probabilities rather than amplitudes and assume that relative phases cancel the interference on average. However, interference effects can play an important role for the dilepton production. In the present model the decay of nuclear resonances which is the dominant source for the dilepton yield, requires the destructive interference of intermediate ρ and ω mesons with their excited states. The interference can at least partially be destroyed by the presence of the medium which leads to an enhancement of the corresponding dilepton yield (Fig. 3). We proposed a scheme to treat the decoherence in the medium on a microscopic level.

Predictions for the HADES experiment, i.e. dilepton spectra in C+C reactions at 1 and 2 AGeV from [32] are shown in Fig. 4. Besides the dilepton spectrum with in-vacuum properties of the intermediate mesons (depicted by a dashed line) the effects of three different in-medium scenarios on the same spectrum are also shown. The calculation in which all the in-medium effects are included to their full extent is depicted by a full line. For this scenario the widths of the ω and ρ mesons have been chosen $\Gamma_\omega = 200$ MeV and respectively $\Gamma_\rho = 300$ MeV, together with the inclusion of Brown-Rho scaling for the

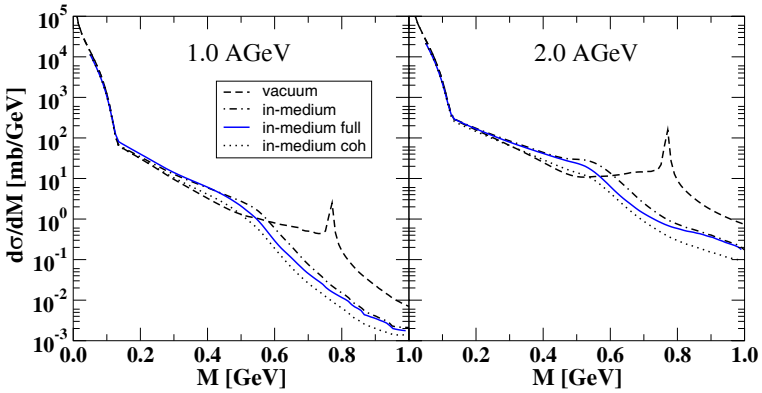

Fig. 5 – Dilepton spectrum in C+C at 1 AGeV (left panel) and 2 AGeV (right panel). Besides the vacuum calculation (dashed line) three different scenarios for the in-medium modification of the dilepton yield are presented. The full in-medium calculation (full line) takes into account Brown-Rho scaling for the vector meson masses, collisional broadening ($\Gamma_\rho = 300$ MeV, $\Gamma_\omega = 200$ MeV) and decoherence effects. The two extra in-medium calculations differ from the full one in a few respects: $\Gamma_\rho = 150$ MeV (vacuum value) for the dashed-dotted curve and no decoherence effects for the dotted line.

meson masses and decoherence effects. The remaining two calculations provide insight on the significance of the individual in-medium effects, even tough strictly speaking they cannot be disentangled. The variation of the ρ meson width between $\Gamma_\rho = 150 \ldots 300$ MeV leads to a modification of the dilepton yield by a factor of 2 in the dilepton mass range $0.5 - 0.8$ GeV (compare the full and dashed-dotted curves). Decoherence effects in nuclear medium are responsible for at most a 50 % change in the dilepton differential cross section at intermediate dilepton masses (dotted and full lines). The effect of the Brown-Rho scaling is well known: it produces a shift of the ρ/ω peak from its vacuum position towards lower dilepton invariant masses, namely around 0.6 GeV. The peak dissolves once the width of the ω meson is changed to its in-medium value. All results have been obtained with a strong $N^*(1535)N\omega$ coupling as enforced by the fit of the resonance model parameter to nucleon resonance electro- and photo-production [21] and which has been used in [17, 26].

The results of Fig. 5 are pure theoretical results, i.e. they have not been filtered in order to account for the experimental detector acceptance. Such a procedure is, however, indispensable for a meaningful comparison to data. In order to investigate up to what degree the HADES experiment will be able to discriminate between the different scenarios, we apply in the following the full HADES acceptance filter in combination with a smearing procedure for the corresponding HADES mass resolution. The filtered results are shown in

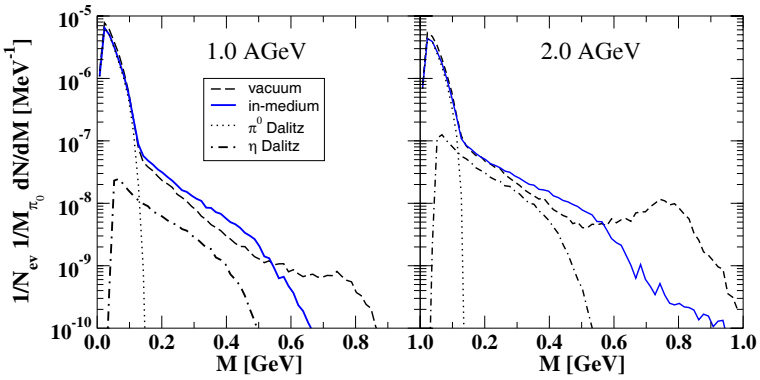

Fig. 6 – Dilepton spectrum in C+C reactions at 1.0 and 2.0 AGeV after application of the full HADES acceptance filter. Calculations without (vacuum) and including in-medium effects (in-medium), i.e. ρ and ω collisional broadening and mass shifts and decoherence, are shown.

Fig. 6. The "in-medium" calculation contains the combination of all medium effects under consideration, i.e. ρ and ω collisional broadening and mass shifts and decoherence (corresponding to the full lines in Fig. 5). The spectra are normalized to the number of events $N_{\rm ev}$ and to the π^0 multiplicity. Contributions from π^0 and η Dalitz decay are shown separately. The difference between the "vacuum" and the "in-medium" calculation is still clearly visible: most pronounced are the medium effects in the mass region around the ρ/ω peak ($M \sim 0.6 \div 1$ GeV) where a complete dissolution of the ρ and in particular the ω peak is predicted. This effect is even more pronounced at 2 AGeV and the HADES experiment will be able to clearly discriminate between the "vacuum" and the "in-medium" scenario.

In the low and intermediate mass region the medium effects are less pronounced, i.e. of the order of about 50 %. Decoherence affects the dilepton pairs over almost the entire spectrum. It is, however, the only source for "in-medium" changes at low invariant dilepton masses, below 0.4 GeV. To discriminate the various scenarios experimentally in the low and intermediate mass region will be difficult, at least in the light C+C system.

4. CONCLUSIONS

In this paper we have presented predictions for the dilepton emission in heavy ion reactions at C+C at 1 and 2 AGeV. Experimental data for these two reactions will be available in the near future from the HADES Collaboration at GSI. A clear distinction between "vacuum" and "in-medium" scenarios for ρ and ω properties is possible in the mass region around the ρ/ω peak. In particular at 2 GeV the effect from an in-medium broadening of the vector

mesons is dramatic and leads to a strong suppression of the spectrum. At low invariant masses the in-medium effects, in particular the decoherence, are less pronounced, i.e. on the 20-30 % level, but can be expected to be more clearly seen in larger systems than C+C.

Acknowledgements. We would like to acknowledge the help of our experimental colleagues from HADES who have filtered the results of our model with the HADES filter.

REFERENCES

1. G.E. Brown, M. Rho, Phys. Rev. Lett., **66**, 2720 (1991); Phys. Rep., **269**, 333 (1996).
2. T. Hatsuda, S.H. Lee, Phys. Rev., **C46**, R34 (1992); I. Koike, *ibid.*, **51**, 1488 (1995); T. Hatsuda, S.H. Lee, H. Shiomi, *ibid.*, **52**, 3364 (1992); S. Leuopold, *ibid.*, **64**, 015202 (2001); S. Zschoke, O.P. Pavlenko, B. Kämpfer, Eur. Phys. J., **A15**, 529 (2002).
3. C.M. Shakin, W.D. Sun, Phys. Rev., **C49**, 1185 (1994); M. Asakawa, C.M. Rho, Phys. Rev., **C48**, R526 (1993); N. Kaiser, W. Weise, Nucl. Phys., **A624**, 527 (1997).
4. M. Hermann, B. Friman, W. Nörenberg, Nucl. Phys., **A560**, 411 (1993); G. Chanfray, P. Schuck, Nucl. Phys., **A545**, 271c (1992); R. Rapp, G. Chanfray, J. Wambach, Nucl. Phys., **A617**, 472 (1997).
5. B. Friman, H.J. Pirner, Nucl. Phys., **A617**, 496 (1997).
6. G. Agakichiev *et al.* [CERES Collaboration], Phys. Rev. Lett., **75**, 1272 (1995).
7. A. Marin, *et al.* [CERES Collaboration], J. Phys., **G30**, S709 (2004).
8. M.A. Mazzoni, Nucl. Phys., **A566**, 95c (1994); M. Masera, Nucl. Phys., **A590**, 93c (1995).
9. S. Damjanovic *et al.* [NA60 Collaboration], J. Phys., **G31**, S903 (2005).
10. W. Cassing, W. Ehehalt, C.M. Ko, Phys. Lett., **B363**, 35 (1995); G.Q. Li, C.M. Ko, G.E. Brown, Nucl. Phys., **A606**, 568 (1996); C.M. Hung, E.V. Shuryak, Phys. Rev., **C56**, 453 (1997).
11. M. Urban, M. Buballa, R. Rapp, J. Wambach, Nucl. Phys., **A641**, 433 (1998); Nucl. Phys., **A673**, 357 (2000); R. Rapp, J. Wambach, Adv. Nucl. Phys., **25**, 1 (2000).
12. E.L. Bratkovskaya, W. Cassing, R. Rapp, J. Wambach, Nucl. Phys., **A634**, 168 (1998).
13. D. Trnka *et al.* [CBELSA/TAPS Collaboration], Phys. Rev. Lett., **94**, 192303 (2005).
14. R.J. Porter *et al.* [DLS Collaboration], Phys. Rev. Lett., **79**, 1229 (1997).
15. W.K. Wilson *et al.* [DLS Collaboration], Phys. Rev., **C57**, 1865 (1998).
16. C. Ernst, S.A. Bass, M. Belkacem, H. Stöcker, W. Greiner, Phys. Rev., **C58**, 447 (1998); E.L. Bratkovskaya, C.M. Ko, Phys. Lett., **B445**, 265 (1999).
17. K. Shekhter, C. Fuchs, A. Faessler, M. Krivoruchenko, B. Martemyanov, Phys. Rev., **C68**, 014904 (2003).
18. $***$, HADES Collaboration, private communication.
19. J. Friese, HADES Collaboration, Prog. Part. Nucl. Phys., **42**, 235 (1999).
20. A. Faessler, C. Fuchs, M.I. Krivoruchenko, Phys. Rev., **C61**, 035206 (2000).
21. M.I. Krivoruchenko, B.V. Martemyanov, A. Faessler, C. Fuchs, Ann. Phys., **296**, 299 (2002).
22. A. Faessler, C. Fuchs, M.I. Krivoruchenko, B.V. Martemianov, J. Phys., **G29**, 603 (2003).
23. M. Post, U. Mosel, Nucl. Phys., **A688**, 808 (2001).

24. A.I. Vainstein, V.I. Zakharov, Phys. Lett., **B72**, 368 (1978).
25. S.J. Brodsky, G.R. Farrar, Phys. Rev. Lett., **31**, 1153 (1973); S.J. Brodsky, G.R. Farrar, Phys. Rev., **C11**, 1309 (1975).
26. C. Fuchs *et al.*, Phys. Rev., **C67**, 025202 (2003).
27. F. Hibou *et al.*, Phys. Rev. Lett., **83**, 492 (1999); COSY-TOF Collaboration, Phys. Lett., **B522** , 16 (2001); F. Balestra *et al.*, Phys. Rev., **C63**, 024004 (2001).
28. A. Faessler, C. Fuchs *et al.*, Phys. Rev., **C70**, 035211 (2004).
29. C. Ernst *et al.*, Phys. Rev., **C58**, 447 (1998).
30. E.L. Bratkovskaya, W. Cassing, U. Mosel, Nucl. Phys., **A686**, 568 (2001).
31. E.L. Bratkovskaya, W. Cassing, R. Rapp, J. Wambach, Nucl. Phys., **A634**, 168 (1998).
32. M.D. Cozma, C. Fuchs, E. Santini, A. Faessler, nucl-th/0601059.